Korean J. Chem. Eng., **31**(9), 1547-1552 (2014)
DOI: 10.1007/s11814-014-0087-2

pISSN: 0256-1115
eISSN: 1975-7220

Investigation on the morphology of hierarchical mesoporous ZSM-5 zeolite prepared by the CO_2-in-water microemulsion method

Chunlei Wang*, Jianfen Li*, Juntao Yan*,†, and Jianmin Sun**

*College of Chemistry and Environmental Engineering, Wuhan Polytechnic University, Wuhan 430023, China
**State Key Lab of Urban Water Resource and Environment, Harbin Institute of Technology, Harbin 150090, China
(*Received 7 December 2013 • accepted 22 March 2014*)

Abstract−A series of hierarchical mesoporous ZSM-5 zeolites with different morphology were successfully synthesized by the CO_2-in-water microemulsion method, and mesoporosity was formed without organotemplate. The different synthesis conditions, including silica alumina molar ratio, stirring time and compressed CO_2 pressure, were systematically investigated to discuss the influence of these conditions on the morphology of ZSM-5 zeolite. The resulting samples were characterized by scanning electron microscopy (SEM), X-ray diffraction (XRD), inductively coupled plasma (ICP) and nitrogen adsorption-desorption measurement. XRD results indicated that compressed CO_2 route for the synthesis of MFI zeolites had a fast crystallization rate and good crystallinity. SEM images showed that the ZSM-5 hierarchical mesoporous ZSM-5 zeolite had a uniform chain-like crystal morphology, whereas silicalite-1 displayed a monodisperse crystal morphology. In addition, the nitrogen adsorption-desorption measurement provided sufficient evidence for the presence of hierarchical mesopores in ZSM-5 zeolite.

Keywords: CO_2-in-water Microemulsion, Chain-like, Morphology, Hierarchical Mesoporous, ZSM-5

INTRODUCTION

As is known, zeolites are important solid acid catalytic materials that have widespread applications in the petroleum refining, coal chemical industry and fine chemical industries [1-5]. These materials possess various catalytically desirable properties, such as high surface area, adjustable pore size, acidity and high thermal and hydrothermal stability [6]. However, their relatively small and uniform micropores seriously influence the mass transfer of reactants and products, thereby reducing the catalytic conversion of bulky molecules [4,7-9]. One way to overcome these limitations is to prepare mesoporous zeolites [10-15]. For example, hierarchical mesoporous zeolites have been synthesized using a mixture of small organic ammonium salts and mesoscale cationic polymers through the template method [8]. Mesoporous ZSM-5 have been obtained by crystallization of aged gels in the presence of cetyltrimethylammonium cations [10]. Organic-functionalized mesoporous ZSM-5 zeolites have been prepared by consecutive desilication and silanization [11].

Emulsion templating is one of the most effective approaches for the preparation of highly porous materials and mesoporous macroscale structures [16], such as organic polymers [17-23], inorganic materials [24-26], and inorganic-organic composites [27,28]. During the last several years, due to the unique properties such as nontoxicity, nonflammability, high diffusivity, low viscosity, and natural abundance [29-32], the templating of CO_2-in-water emulsion has been successfully used in the synthesis and processing of porous materials, such as porous polymer [16,33-36], organic small molecular porous materials [33], inorganic porous materials and so on [37-39]. For example, Butler et al. obtained highly porous emulsion-templated materials via the polymerization of concentrated CO_2-in-water (C/W) emulsions [16]. Wang et al. achieved mesoporous silica hollow spheres from CO_2-in-water emulsion templating in the presence of non-ionic block copolymers [38]. Wakayama et al. synthesized microporous and mesoporous metal oxides which replicate both the macroscopic shapes and nanoscale structures of activated carbon templates via supercritical CO_2 [40].

In our previous work, we developed a new approach to the synthesis of MFI zeolites which possessed a fast crystallization rate and hierarchical mesopores in the presence of CO_2-in-water microemulsions, and mesoporosity was formed without organotemplate [41]. Herein, we systematically investigated the effects of synthesis conditions on the morphology of ZSM-5-S (the synthesis of ZSM-5 zeolites in the presence of compressed CO_2 was designated as ZSM-5-S) by the CO_2-in-water microemulsion method, such as different silica alumina molar ratio, stirring time and pressure, and so on. By the characterization of SEM, the length of chain-like crystal morphology increased with the decreasing of silica alumina molar ratio. And the different stirring time had an effect on the crystal morphology. In addition, the pore volume was relative to the pressure of compressed CO_2. The systematic investigation results of synthesis conditions and morphology of ZSM-5-S zeolite provided us a guide for catalytic cracking experiments in the next stage.

EXPERIMENTAL

1. Materials

Tetrapropylammonium hydroxide (TPAOH) and aluminum iso-

†To whom correspondence should be addressed.
E-mail: yanjuntaonihao@163.com

propoxide were purchased from Tianjin Guangfu Chemical Reagents Company, China. NaOH and NH_4F (Beijing Chemical Reagent Company, China) was of reagent grade. The water used was distilled followed by deionization.

2. Synthesis of Chain-like ZSM-5 Zeolite in the Presence of Compressed CO_2

A typical synthesis procedure of ZSM-5 zeolite in the presence of compressed CO_2 was as follows: 6.25 mL of tetraethyl orthosilicate (TEOS), 10 mL of tetrapropylammonium hydroxide (TPAOH, 10.7 wt%), and 1.5 mL of NaOH aqueous solution (1 M) were mixed first, and then the desired amount of aluminum isopropoxide was added at room temperature. After stirring for 8 h, the mixture was transferred into 50 mL stainless steel autoclave at 150 °C with oil bath heating. Thereafter, the pressure of CO_2 in the autoclave was charged up to the expected pressure with high-pressure liquid pump, and the mixture was further crystallized at 150 °C for 8 h. After filtration, the achieved products were dried at room temperature and calcined at 550 °C for 4 h. This sample was designated as ZSM-5-S.

We also synthesized ZSM-5 zeolite in the presence of fluoride ion via compressed CO_2. The detailed molar ratio of SiO_2 : Al_2O_3 : TPABr : H_2O : NH_4F was 1 : 0.02 : 0.23 : 34 : 0.9. This sample was designated as F-ZSM-5-S. For comparison, conventional ZSM-5 and F-ZSM-5 zeolites were synthesized under the same conditions except for the absence of CO_2.

3. Measurements

X-ray diffraction (XRD) data were collected on a Rigaku D/MAX 2550 diffractometer with Cu Kα radiation. Nitrogen adsorption-desorption isotherms at 77 K were measured using a Micromeritics ASAP 2010M system. The samples were degassed for 10 h at 300 °C before the measurement. Scanning electron microscopy (SEM) experiments were performed on JEOL electron microscopes (FE-JSM6700, Japan). Inductively coupled plasma (ICP) was measured on Perkin-Elmer 3300 DV.

Table 1. Synthesis conditions of ZSM-5-S zeolites in the different figures

Sample of ZSM-5-S	Si/Al molar ratio	Stirring time, h	Pressure, MPa	Crystallization time, h
Fig. 1	23.4	8	8	8
Fig. 2	--	8	8	8
Fig. 3	39.1	--	8	8
Fig. 4	39.1	8	--	8

RESULTS AND DISCUSSION

1. Morphology of ZSM-5-S Synthesized Under the Different Reaction System

To systematically analyze the formation reasons of chain-like crystal morphology, we synthesized ZSM-5 zeolites under a different reaction system, including compressed CO_2, N_2 atmosphere and conventional synthesis system. The effects of different silica alumina molar ratio, stirring time and pressure on ZSM-5-S were also investigated. The detailed synthesis conditions of ZSM-5-S zeolites in the different figures are summarized in Table 1.

In the present work, the morphology of ZSM-5-S was characterized by SEM. And SEM images (Fig. 1(a), (b), (c)) at different magnifications exhibited high purity of crystalline phase, which was in agreement with the XRD results. However, surprisingly and interestingly, conventional zeolite had a monodisperse crystal morphology with an average diameter of 300 nm (Fig. 1(d)), while ZSM-5-S (Fig. 1(a), (b), (c)) showed a uniform chain-like crystal morphology with a length of about 2 μm and an average diameter of 450 nm.

Taking into account the effect of CO_2 pressure on the chain-like crystal morphology, we also synthesized ZSM-5 according to the above procedure in N_2 atmosphere instead of CO_2. By the charac-

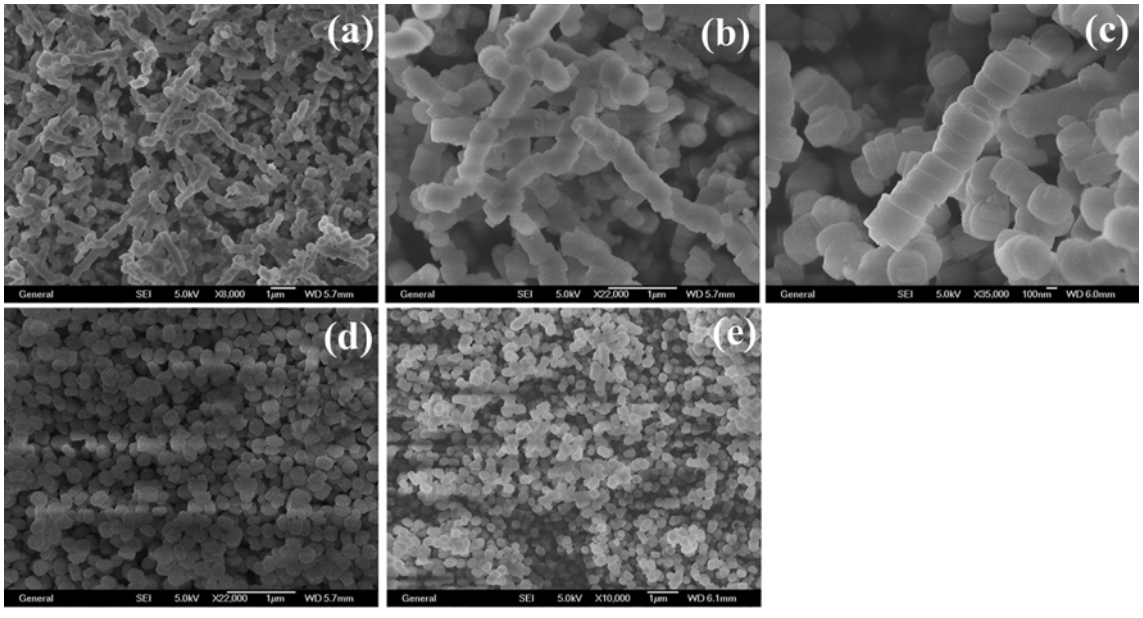

Fig. 1. SEM images of ((a), (b) and (c)) ZSM-5-S synthesized for 8 h in the presence of compressed CO_2 at different magnifications, (d) conventional synthesis of ZSM-5 synthesized for 88 h in the absence of CO_2, (e) ZSM-5 synthesized for 24 h under N_2 atmosphere condition.

Table 2. ICP results of ZSM-5-S zeolites with different amount of aluminium isopropoxide

	1	2	3	4
TEOS (mL)	6.25	6.25	6.25	6.25
Aluminum isopropoxide (g)	0.25	0.15	0.063	0
Theory values-Si/Al molar ratio	22.8	38.2	90.5	--
ICP results-Si/Al molar ratio	23.4	39.1	91.5	--

terization of SEM (Fig. 1(e)), ZSM-5 achieved in N_2 atmosphere displayed a monodisperse crystal morphology rather than a chain-like crystal morphology that ZSM-5-S possessed, which fully demonstrated that the compressed CO_2 played an important role in the formation of a chain-like crystal morphology.

2. Morphology and ICP Results of ZSM-5-S Synthesized with Different Amount of Aluminum Isopropoxide

By varying the silica alumina molar ratio, a series of samples with different amount of aluminum isopropoxide were synthesized under the given procedure, such as 0.25 g, 0.15 g, 0.063 g, and even 0 g. The silica alumina molar ratio in samples was determined by inductively coupled plasma analysis (ICP), which was consistent with the theory values. The ICP results of ZSM-5-S zeolites with different amount of aluminum isopropoxide are summarized in Table 2.

Based on the SEM images (Fig. 2), when the amount of aluminum isopropoxide was 0.25 g (Fig. 2(a)), 0.15 g (Fig. 2(b)), 0.063 g (Fig. 2(c)), the lengths of chain-like crystal were about 2 μm, 1 μm and 0.5 μm, respectively. It was concluded that the length of chain-like crystal morphology shortened with the decreasing aluminum isopropoxide amount. In the case of aluminum isopropoxide, the amount decreased to 0.063 g, and the length of chain-like crystal was not uniform. Particularly, when the sample was synthesized without aluminum isopropoxide, it clearly showed a monodisperse crystal morphology rather than a chain-like crystal morphology. In a word, the amount of aluminum isopropoxide also played a role in the formation of chain-like crystal morphology.

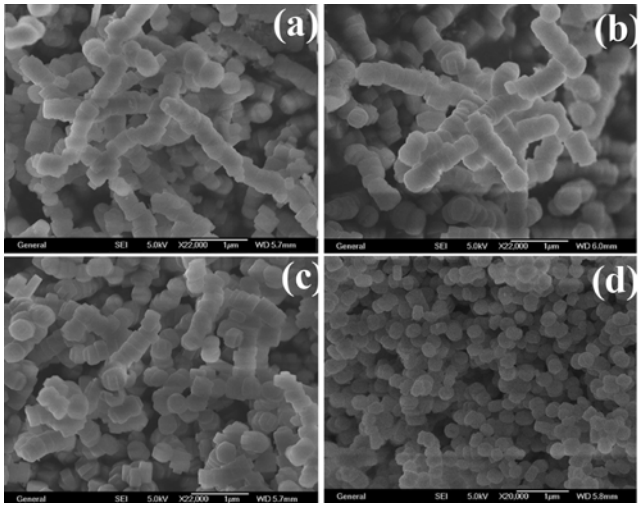

Fig. 2. SEM images of ZSM-5-S synthesized with different amount of aluminum isopropoxide: (a) 0.25 g, (b) 0.15 g, (c) 0.063 g, (d) 0 g.

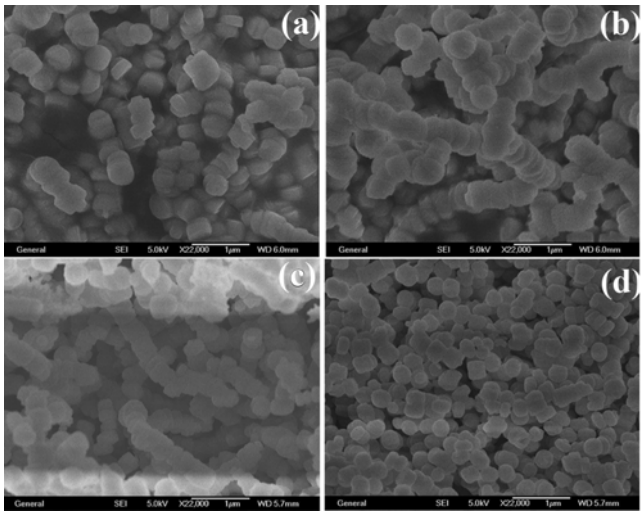

Fig. 3. SEM images of ZSM-5-S with different stirring time (a) 2 h, (b) 5 h, (c) 8 h, (d) 15 h, and synthesized for 8 h in the presence of compressed CO_2.

3. Morphology of ZSM-5-S Synthesized with Different Stirring Time and Compressed CO_2 Pressure

ZSM-5-S was synthesized according to the above procedure with different stirring time. Based on the SEM images (Fig. 3), at a given stirring time of 2 h (Fig. 3(a)), there was not obvious chain-like structure, but three crystals connected together. At a given stirring time of 5 h, a chain-like crystal morphology was observed (Fig. 3(b)). When the stirring time increased to 8 h (Fig. 3(c)), it showed an obvious chain-like crystal morphology, and the length was about 1.5 μm. However, at 15 h, the chain-like crystal morphology was not observed (Fig. 3(d)), no matter how long the crystallization time was. These results indicated that stirring time had a distinct effect on the formation of the chain-like crystal morphology, which might be attributed to the effect of starting gel composition on the structure of aluminosilicate.

In addition, based on the SEM images (Fig. 4), when the pressure of compressed CO_2 increased to 15 MPa and 20 MPa, respectively, the length of chain-like crystal was about 1ìm, which was consistent with the sample of ZSM-5-S-8MPa (Fig. 2(b)). It was concluded that the pressure did not have a significant impact on the length of chain-like crystal morphology.

4. XRD Analysis of ZSM-5

The XRD pattern of ZSM-5 zeolites (Fig. 5(a)) and ZSM-5-S crystallized under the different pressure of CO_2, such as 8 MPa (b),

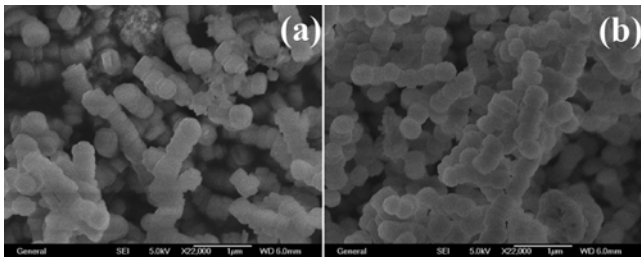

Fig. 4. SEM images of ZSM-5-S crystallized for 8 h in the presence of compressed CO_2 at (a) 15 MPa, and (b) 20 MPa.

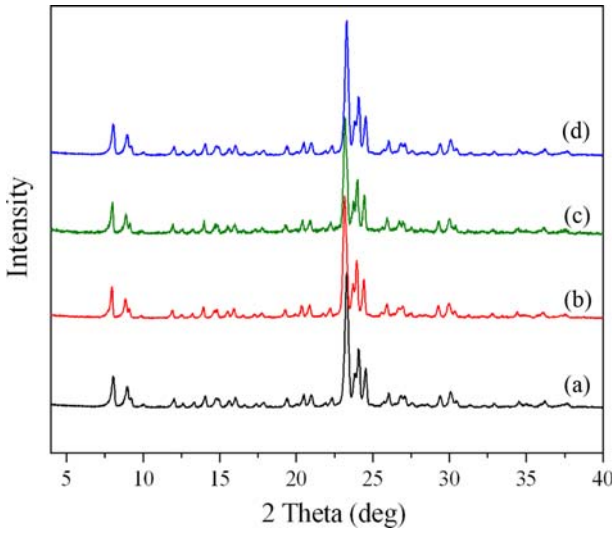

Fig. 5. XRD patterns of (a) conventional ZSM-5 crystallized for 88 h in the absence of CO_2, ZSM-5-S crystallized for 8 h in the presence of compressed CO_2 at 8 MPa (b), (c) 15 MPa, and (d) 20 MPa.

15 MPa (c), and 20 MPa (d), are shown in Fig. 5. Based on Fig. 5, a typical structure of MFI zeolites was observed, which suggested that the MFI structure of ZSM-5-S was not damaged under the high pressure of CO_2. Meanwhile, the crystallization of ZSM-5-S took very short time (8 h) compared with conventional synthesis of ZSM-5 with similar crystallinity (88 h). It was proved that compressed CO_2 route for the synthesis of MFI zeolites had a fast crystallization rate and good crystallinity.

5. N_2 Adsorption-desorption Characterization of ZSM-5

The N_2 adsorption-desorption isotherms and the BJH pore size distribution for various calcined ZSM-5 zeolites are presented in Figs. 6 and 7. As can be observed in Figs. 6A and 7A, the isotherms of various ZSM-5 were of type IV, and displayed an obvious hysteresis loop at relatively high pressure (0.75-1.0) that was assigned to the presence of hierarchical mesopores. Moreover, the

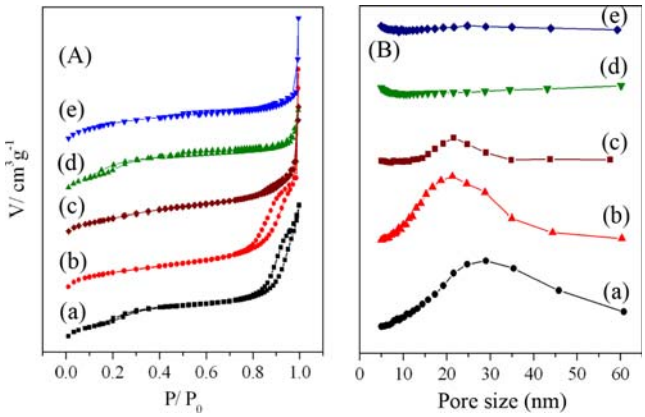

Fig. 6. (A) N_2 adsorption-desorption isotherms and (B) pore size distributions for: (a) ZSM-5-S-8MPa synthesized under compressed CO_2, (b) ZSM-5-S-15MPa synthesized under compressed CO_2, (c) ZSM-5-S-20MPa synthesized under compressed CO_2, (d) ZSM-5-N_2-8MPa synthesized under N_2, (e) Conventional ZSM-5 synthesized for 88 h in the absence of CO_2.

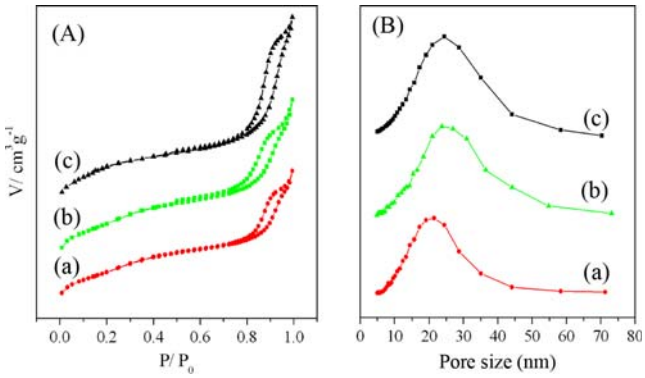

Fig. 7. (A) N_2 adsorption-desorption isotherms and (B) pore size distributions for ZSM-5-S with different stirring time (a) 2 h, (b) 5 h, (c) 15 h, and synthesized in the presence of compressed CO_2.

Table 3. The textural properties of various ZSM-5 zeolites

Sample	Si/Al ratio	Stirring time, h	S[a], m^2/g	V_{total}[b] cm^3/g	V_{meso}[c], cm^3/g	D_{meso}[d], nm
ZSM-5-S-8MPa	23.4	8	322	0.21	0.12	10-40
ZSM-5-S-8MPa[e]	39.1	8	315	0.25	0.14	10-40
ZSM-5-S-8MPa	91.5	8	316	0.23	0.15	10-40
ZSM-5-S-8MPa	39.1	2	334	0.17	0.07	10-40
ZSM-5-S-8MPa	39.1	5	311	0.20	0.12	10-40
ZSM-5-S-8MPa	39.1	15	329	0.23	0.14	10-40
ZSM-5-S-15MPa[e]	39.1	8	327	0.35	0.24	10-40
ZSM-5-S-20MPa	39.1	8	328	0.21	0.10	10-40
ZSM-5-N_2-8MPa[e]	39.1	8	334	0.16	0.08	--
Conventional ZSM-5[e]	39.1	8	369	0.21	0.09	--

[a]BET surface area
[b]Total pore volume at P/P_0=0.95
[c]Pore volume estimated by *t*-plots method
[d]Pore size distribution obtained from BJH analysis by adsorption branch
[e]Obtained from the previous paper results [41]

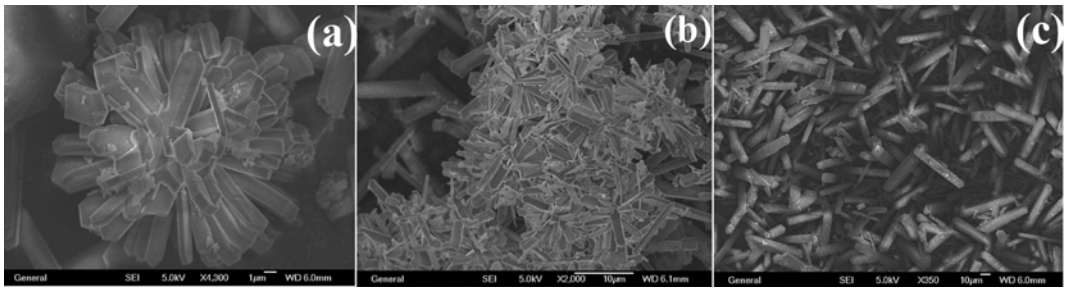

Fig. 8. SEM images of F-ZSM-5-S (a), (b) synthesized for 24 h in the presence of compressed CO_2; (c) conventional F-ZSM-5 crystallized for 72 h in the absence of CO_2.

samples' mesopore size distributions were estimated at about 10-40 nm by using Barrett-Joyner-Halenda (BJH) analyses from the adsorption curve of the isotherms (Fig. 6B, 7B), and the BET surface area was calculated by using the Barrett-Emmett-Teller (BET) method. In contrast, there was no obvious hysteresis loop at relative pressure around P/P_0=0.8-1.0 for ZSM-5 zeolite synthesized under N_2 at the pressure of 8 MPa (Fig. 6A-(d)), which was similar to the conventional zeolite (Fig. 6A-(e)). These results suggested that the formation of mesoporosity in MFI zeolites was closely related to the presence of CO_2-in-water emulsions and foams as templates, which were stabilized by silica species during the synthesis [39]. Particularly so, when the pressure of CO_2 increased from 8 MPa to 15 MPa, and the corresponding pore volume in ZSM-5-S remarkably increased. However, when the pressure of CO_2 increased to 20 MPa, the corresponding pore volume decreased. It might because excessive high pressure damaged the structure of CO_2-in-water emulsions. The textural properties of various ZSM-5 zeolites are summarized in Table 3.

6. Morphology and XRD Analysis of F-ZSM-5-S Synthesized with or without Compressed CO_2

ZSM-5 large single crystal was obtained in the presence of fluoride ion under compressed CO_2. By the characterization of SEM for F-ZSM-5-S and F-ZSM-5 samples, comparisons were made between the F-ZSM-5-S and the conventional F-ZSM-5; interestingly, a flowerlike crystal morphology (Fig. 8(a) and (b)) was observed for F-ZSM-5-S sample rather than a conventional bar-like crystal morphology (Fig. 8(c)). And the length of conventional F-ZSM-5 was about 80 μm, whereas F-ZSM-5-S was only about 12 μm. This result suggested that compressed CO_2 played a critical role in the formation of the flowerlike crystal morphology, and this phenomenon might be attributed to the coacervation that resulted from crystal surface with the aid of CO_2.

The XRD pattern of F-ZSM-5-S zeolite (Fig. 9(a)) showed a typical structure of MFI zeolites; meanwhile, the crystallization of F-ZSM-5-S under compressed CO_2 condition (Fig. 9(a)) took very short time compared with conventional syntheses of F-ZSM-5 with similar crystallinity (Fig. 9(b)).

7. Ammonia Temperature-programmed Desorption of ZSM-5-S

The acidity of ZSM-5-S-15MPa with an Si/Al ratio of 39.1 was determined by means of ammonia temperature-programmed desorption (NH_3-TPD); three NH_3 desorption peaks are observed in Fig. 10. The peak centered at about 251 °C was assigned to the existence of weak acid site, a broad NH_3 desorption peak centered at

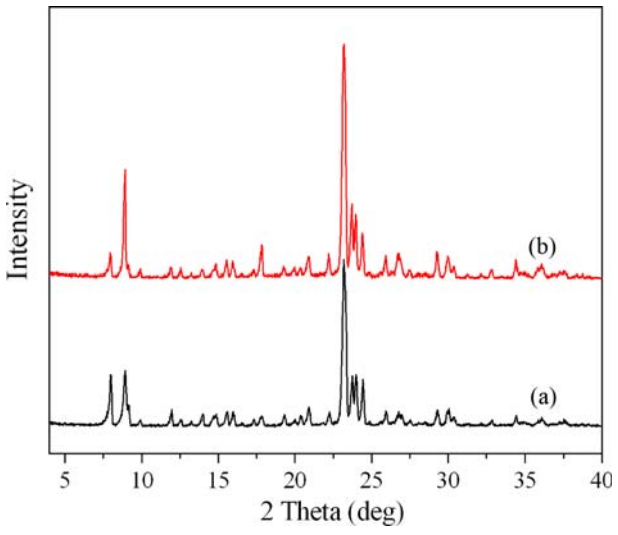

Fig. 9. XRD patterns of (a) F-ZSM-5-S synthesized for 24 h in the presence of compressed CO_2, (b) conventional F-ZSM-5 crystallized for 72 h in the absence of CO_2.

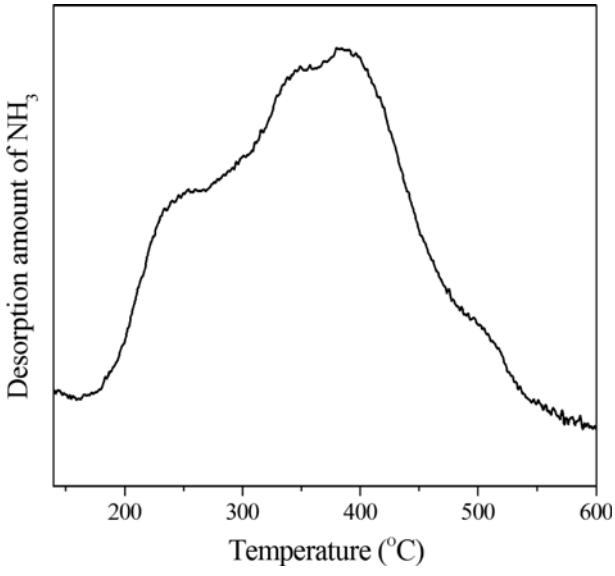

Fig. 10. NH_3-TPD profile of ZSM-5-S-15MPa with an Si/Al ratio of 39.1 synthesized by the CO_2-in-water microemulsion method.

about 390 °C represented the medium acid site, and the peak centered at about 501 °C was attributed to the strong acid site. These results indicated that ZSM-5-S combined the strong acid feature of microporous zeolite with the large pore size feature of mesoporous zeolite; thus ZSM-5-S exhibited potential superiority in the catalytic reaction of bulky molecules.

CONCLUSIONS

We synthesized a series of hierarchical mesoporous ZSM-5 zeolite with different morphology in the presence of CO_2-in-water emulsions. Mesoporosity was formed in the zeolite without using organic mesoporous templates. And effects of synthesis conditions on the morphology of hierarchical mesoporous ZSM-5-S zeolite were systematically investigated. XRD results proved that a compressed CO_2 route for the synthesis of MFI zeolites had a fast crystallization rate and good crystallinity compared to the conventional synthesis method. SEM images showed that the hierarchical mesoporous ZSM-5-S zeolite had a uniform chain-like crystal morphology, whereas silicalite-1 displayed a monodisperse crystal morphology. Based on the SEM images, the length of chain-like crystal morphology increased with the decreasing of silica alumina molar ratio; stirring time also had an effect on the morphology of ZSM-5-S zeolite. These influence factors played important roles in the formation of the chain-like crystal morphology. In addition, the formation mechanism of chain-like crystal morphology of ZSM-5-S zeolite was fully interpreted by discussing the influence of different synthesis conditions on the morphology of ZSM-5 zeolite.

ACKNOWLEDGEMENTS

This study was supported by the Scientific Research Initial Fund for the Introduced Talent of Wuhan Polytechnic University (No. 2013RZ01 and 2013RZ02).

REFERENCES

1. M. Alyani, J. Towfighi and S. M. Sadrameli, *Korean J. Chem. Eng.*, **28**, 1351 (2011).
2. A. Jodaei, A. Niaei and D. Salari, *Korean J. Chem. Eng.*, **28**, 1665 (2011).
3. J. K. Jeon and Y. K. Park, *Korean J. Chem. Eng.*, **29**, 196 (2012).
4. C. J. H. Jacobsen, C. Madsen, J. Houzvicka, I. Schmidt and A. Carlsson, *J. Am. Chem. Soc.*, **122**, 7116 (2000).
5. N. Zeeshan, X. P. Tang and W. Fei, *Korean J. Chem. Eng.*, **26**, 1528 (2009).
6. K. Iwakai, T. Tago, H. Konno, Y. Nakasaka and T. Masuda, *Micropor. Mesopor. Mater.*, **141**, 167 (2011).
7. A. Taguchi and F. Schuth, *Micropor. Mesopor. Mater.*, **77**, 1 (2005).
8. F. S. Xiao, L. Wang, C. Yin, K. Lin, Y. Di, J. Li, R. Xu, D. S. Su, R. Schlögl, T. Yokoi and T. Tatsumi, *Angew. Chem. Int. Ed.*, **45**, 3090 (2006).
9. H. Wang and T. J. Pinnavaia, *Angew. Chem. Int. Ed.*, **45**, 7603 (2006).
10. M. L. Gonçalves, L. D. Dimitrov, M. H. Jordão, M. Wallau and E. A. Urquieta-González, *Catal. Today*, **133**, 69 (2008).
11. S. Mitchell, A. Bonilla and J. Pérez-Ramírez, *Mater. Chem. Phys.*, **127**, 278 (2011).
12. A. Janssen, *Micropor. Mesopor. Mater.*, **65**, 59 (2003).
13. Y. Tao, H. Kanoh and K. Kaneko, *J. Am. Chem. Soc.*, **125**, 6044 (2003).
14. Y. S. Tao, H. Kanoh, Y. Hanzawa and K. Kaneko, *Colloids Surf. A*, **241**, 75 (2004).
15. L. Wang, C. Yin, Z. Shan, S. Liu, Y. Du and F.-S. Xiao, *Colloids Surf. A*, **340**, 126 (2009).
16. R. Butler, I. Hopkinson and A. I. Cooper, *J. Am. Chem. Soc.*, **125**, 14473 (2003).
17. N. R. Cameron and D. C. Sherrington, *Adv. Polym. Sci.*, **126**, 163 (1996).
18. A. Barbetta, N. R. Cameron and S. J. Cooper, *Chem. Commun.*, **3**, 221 (2000).
19. N. R. Cameron and A. Barbetta, *J. Mater. Chem.*, **10**, 2466 (2000).
20. E. Ruckenstein, *Adv. Polym. Sci.*, **127**, 1 (1997).
21. N. R. Cameron, D. C. Sherrington, L. Albiston and D. P. Gregory, *Colloid Polym. Sci.*, **274**, 592 (1996).
22. J.-Y. Lee, B. Tan and A. I. Cooper, *Macromolecules*, **40**, 1955 (2007).
23. H. Zhang and A. I. Cooper, *Chem. Mater.*, **14**, 4017 (2002).
24. A. Imhof and D. J. Pine, *Nature*, **389**, 948 (1997).
25. A. Imhof and J. Pine, *Adv. Mater.*, **11**, 311 (1999).
26. V. N. Manoharan, A. Imhof, J. D. Thorne and D. J. Pine, *Adv. Mater.*, **13**, 447 (2001).
27. S. M. Klein, V. N. Manoharan, D. J. Pine and F. F. Lange, *Langmuir*, **21**, 6669 (2005).
28. H. Tai, A. Sergienko and M. S. Silverstein, *Polymer*, **42**, 4473 (2001).
29. C. Aymonier, A. Loppinetserani, H. Reveron, Y. Garrabos and F. Cansell, *J. Supercrit. Fluids*, **38**, 242 (2006).
30. A. Cabañas, E. Enciso, M. C. Carbajo, M. J. Torralvo, C. Pando and J. A. R. Renuncio, *Chem. Commun.*, **20**, 2618 (2005).
31. K. Esumi, S. Sarashina and T. Yoshimura, *Langmuir*, **20**, 5189 (2004).
32. R. Sui, A. S. Rizkalla and P. A. Charpentier, *Langmuir*, **22**, 4390 (2006).
33. A. I. Cooper, *Adv. Mater.*, **15**, 1049 (2003).
34. H. H. Winter, G. Gappert and H. Ito, *Macromolecules*, **35**, 3325 (2002).
35. H. Matsuyama, H. Yano, T. Maki, M. Teramoto, K. Mishima and K. Matsuyama, *J. Membr. Sci.*, **194**, 157 (2001).
36. R. Butler, C. M. Davies and A. I. Cooper, *Adv. Mater.*, **13**, 1459 (2001).
37. H. Wakayama and Y. Fukushima, *Ind. Eng. Chem. Res.*, **45**, 3328 (2006).
38. J. Wang, Y. Xia, W. Wang, R. Mokaya and M. Poliakoff, *Chem. Commun.*, **2**, 210 (2005).
39. J. Wang, Y. Xia, W. Wang, M. Poliakoff and R. Mokaya, *J. Mater. Chem.*, **16**, 1751 (2006).
40. H. Wakayama, H. Itahara, N. Tatsuda, S. Inagaki and Y. Fukushima, *Chem. Mater.*, **13**, 2392 (2001).
41. J. M. Sun, C. L. Wang, L. Wang, L. Liang, X. F. Liu, L. Chen and F.-S. Xiao, *Catal. Today*, **158**, 273 (2010).